Electron emission induced by grazing impact of H^+ and He^+ ions on a Cu(001) surface: Low-energy electron diffraction study

T. Bernhard and H. Winter*
Institut für Physik, Humboldt Universität zu Berlin, Brook-Taylor-Strasse 6, D-12489 Berlin-Adlershof, Germany
(Received 5 September 2008; revised manuscript received 13 November 2008; published 26 January 2009)

Electron emission induced by H^+ and He^+ ions with energies up to 30 keV is studied for grazing impact on a clean and flat Cu(001) surface by making use of electron diffraction effects. Depending on the azimuthal orientation of low index directions in the crystal surface with respect to the projectile beam, we observe intensity spots in the angular distributions of emitted electrons. The data are analyzed in the framework of electron diffraction at the ordered surface and reveal interesting details on the emission and coherence mechanisms for the excitation of conduction electrons by fast atomic projectiles in the surface region of a metal.

DOI: 10.1103/PhysRevB.79.033411 PACS number(s): 79.20.Rf

Diffraction phenomena of electrons at solid surfaces play an important role in surface science. The diffraction of low-energy electrons (LEED) is a standard analytical tool for the characterization of ordered structures at crystal surfaces which has reached over the last decades a high level of sophistication concerning studies on complex structures[1] and on the characterization of defects of crystal surfaces.[2] As a further example, we mention the diffraction of photoelectrons at surfaces which provides information on the short-range order for adsorbed species.[3] Whereas for electrons or photons as primary particles a huge body of work can be stated, studies on diffraction of electrons excited by impact of fast atomic projectiles are rare. Early work on diffraction of electrons emitted during ion scattering was reported for large-angle impact of 10–100 kV Ar^+ ions on Ag(111) (Ref. 4) and Cu (Ref. 5). In those experiments, the presence of diffraction effects for secondary electrons was deduced from the variation in the intensity of emitted electrons at fixed energies for the azimuthal rotation of the target surface.

Recently, we performed experiments on electron emission during grazing scattering of fast protons where angular distributions of electrons with defined final energies were recorded.[6] Similar as for conventional LEED, intensity spots were clear-cut signatures for electron diffraction phenomena. In those studies, we also demonstrated that electron spectra recorded at a fixed angle of observation can be modified substantially by diffraction effects. This finding relates closely to the structures in electron spectra which were attributed to the decay of excited bulk and surface plasmons.[7–9] Some of the observed spectral features could be understood also in terms of electron diffraction.[6,10] The disappearance of such spectral structures for ion impact on polycrystalline targets supported this interpretation.[11]

In this Brief Report, we report on detailed studies on the angular distributions of electrons emitted during grazing scattering of light ions from a Cu(001) surface. From the spot patterns observed in our experiments, we derive different features related to the electronic excitation mechanisms present for grazing impact of ions on metal surfaces. We reveal that the coherence length in the quantum-scattering process of electrons here is given by the transport length of electrons in solids.

In our experiments 30 keV H^+ and 25 keV He^+ ions are scattered under a grazing angle of incidence $\Phi_{in}=1.6°$ from a clean and flat Cu(001) surface. The surface is prepared by cycles of grazing sputtering with 25 keV Ar^+ ions and subsequent annealing at temperatures of about 770 K.

The angular distributions of electrons ejected by ion impact are recorded using a commercially available spot profile analysis LEED system (SPA-LEED),[12,13] as sketched in Fig. 1. The acceptance cone of the entrance aperture of the instrument for emitted electron amounts to about $\pm 25°$ with respect to the surface normal. This instrument allows one to obtain angular distributions of electrons emitted from the surface via deflection to the small aperture (0.1 mm) of a channeltron detector by means of an electric octupole field. We used the setup for detection of electrons only, i.e., the electron gun was switched off. Effects of ion-beam fluctuations were reduced by normalization of data to the current of incident ions. A suppressor electrode in the detector unit for reducing contributions of inelastically scattered electrons in conventional LEED allowed us to operate the system as a high pass filter with respect to the electron energies.

As a representative example for the data acquisition, we show in Fig. 2 two-dimensional (2D) distributions for the electron intensities with a resolution of (50×50) pixels, i.e., angle intervals of about $(1°\times 1°)$. In the top panels of Fig. 2 we present two 2D plots for the scattering of 25 keV He^+ ions scattered under a grazing angle of incidence $\Phi_{in}=1.6°$ from a Cu(001) surface along [110]. Selected by means of

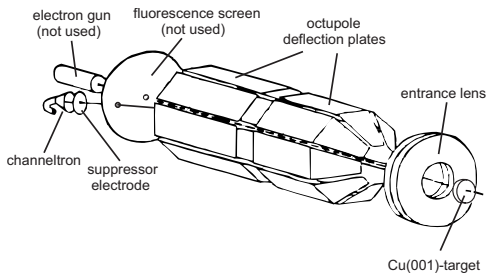

FIG. 1. Sketch of SPA-LEED setup for measurements of energy-resolved angular distributions of electrons emitted during ion impact on metal surface. Electrons are detected by means of channeltron detector. Suppressor electrode in front of detector acts as high pass filter for electron energy. Angular distributions are scanned by means of electric octupole field plates. Electron gun and fluorescence screen for regular LEED operation are not used here (see also Ref. 12).

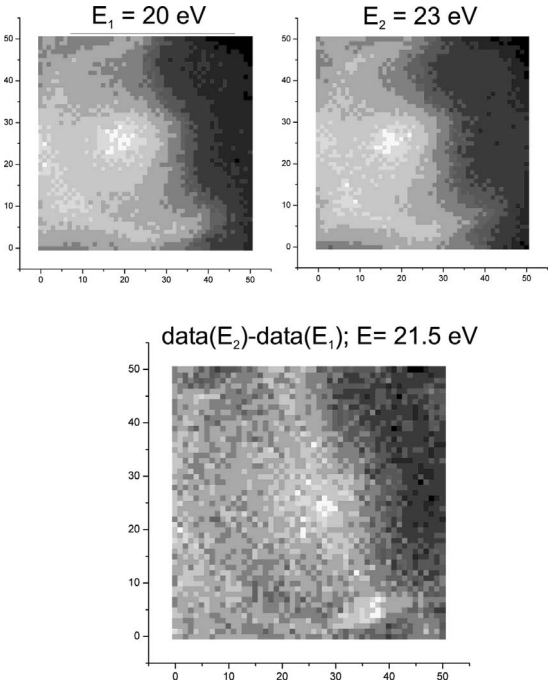

FIG. 2. Upper panel: 2D-intensity distributions for scattering of 25 keV He^+ ions under $\Phi_{in}=1.6°$ from a Cu(001) surface along [110] for electron energies larger than 20 eV (left panel) and 23 eV (right panel). Pixel width corresponds to angle of about 1°. Lower panel: Difference of 2D-intensity distributions shown in upper panel resulting in angular distributions for electron energies of 21.5 ± 1.5 eV. Gray scale: "black"—low intensity; "white"—peak intensity.

the suppressor electrode, the minimum electron energies amount to 21 eV (left panel) and 23 eV (right panel). The 2D plot in the lower panel of Fig. 2 shows the difference of the two data sets, i.e., angular distributions for electrons with mean energies of 21.5 eV and an energy interval of ±1.5 eV. The resulting distribution reveals a prominent spot in the center and two weak spots at the upper and lower rims. In the further processing of the images, a level of about 50%–60% of the peak intensities is set to an incoherent background signal ("black") and in a smoothed and gray-scale representation peak intensities are plotted in "white." Recording of data is fairly elaborate and takes about 1 h in order to accumulate sufficient statistics.

In Figs. 3 and 4 we display the intensity distributions for emitted electrons obtained with 25 keV He^+ ions scattered under $\Phi_{in}=1.6°$ along the low index [110] azimuthal direction of the Cu(001) surface. The data in Fig. 3 are obtained from the difference of measurements with repeller voltages of 43 and 55 eV, i.e., for electron energies of (49 ± 6) eV. Figure 4 shows data for electron energies of (32 ± 5) eV recorded at otherwise same conditions. The white arrow represents the direction of the incident ion beam, where its tip denotes the direction normal to the surface. The distributions reveal pronounced intensity enhancements ("spots") which can be attributed to electron diffraction as outlined below. Note the substantial angular width compared to the bright and sharp spots found in conventional LEED where well-focused beams of electrons with defined energy are used in the incident channel.

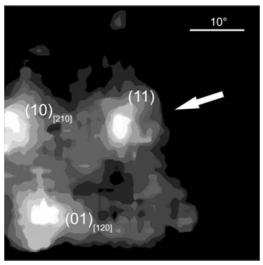

FIG. 3. Difference of 2D-intensity distributions recorded for electron energies of 43 and 55 eV with SPA-LEED for 25 keV He^+ ions scattered under $\Phi_{in}=1.6°$ from Cu(001) along [110]. Arrow indicates the direction of incident beam, tip of arrow direction normal to surface. Lower grayscale level (black) at about 60% of maximum intensity.

Support for the interpretation of data in terms of electron diffraction and the determination of the angular positions of the intensity spots is obtained from concepts of scattering theory using the *Ewald construction* in reciprocal-lattice space.[14] Electrons with initial momentum vectors $\vec{k}_{in}$ oriented along the direction of the incident ion beam are preferentially excited for grazing impact.[15] We follow the suggestions on the production of Bloch waves parallel to the surface by Niehaus *et al.*[10] and derive specific diffraction patterns for elastically scattered electrons that clearly differ from those present for large-angle impact using an electron gun. Owing to the surface potential $[V_o\approx12$ eV for Cu(001) (Ref. 16)], for elastic scattering initial and final momenta change from (atomic units are used) $k_{in}=\sqrt{2(E_e+V_o)}$ to $k_{out}=\sqrt{2E_e}$, with E_e being the final electron energy. Then the condition for intensity spots in the modified Ewald construction scheme in Fig. 5 results from the condition for the scattering vector $\vec{K}=\vec{k}_{out}-\vec{k}_{in}=\vec{G}$ with $\vec{G}$ being a reciprocal-lattice vector.

In Fig. 5 we show a sketch of a plane in reciprocal-lattice space normal (upper panel) and parallel (lower panel) to the surface with the simple square unit cell $\vec{g}_1=\sqrt{2}/a\times[100]$ and $\vec{g}_2=\sqrt{2}/a\times[010]$ with $a=3.61$ Å being the lattice constant of the copper crystal and [100] and [010] is chosen along $\langle1\bar{1}0\rangle$ and $\langle110\rangle$ of the fcc lattice. The solid vertical bars illustrate the Laue conditions for the (00), (11), and (22) reflexes (g_1,g_2). From this construction, the direction of the (11) intensity spot is not too far from the surface normal for electron energies of some tens of eV. Therefore the LEED instrument can be mounted on top of the target surface for the detection of electrons emitted within an angle of some 10° centered around the surface normal.

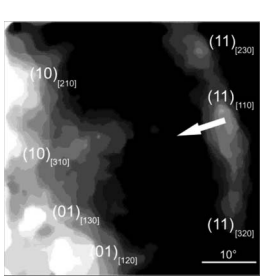

FIG. 4. Same as for Fig. 3, but for the difference of data for electron energies of 27 and 37 eV.

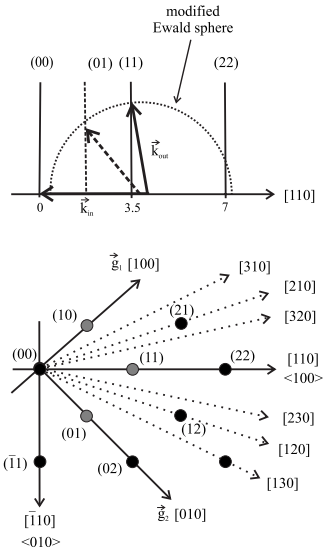

FIG. 5. Ewald construction in reciprocal-lattice space. Upper panel: plane normal to surface; lower panel: plane parallel to surface. Dashed lines indicate directions of higher indexes. Owing to surface potential, momentum vectors k_{in} and k_{out} are different in length.

The polar angles of the intensity spots referred to the surface normal (in beam direction positive angles) are plotted as a function of (final) electron energy in Fig. 6. Electron emission is induced by 25 keV He^+ (full circles) and 30 keV H^+ ion (full triangles) impact under $\Phi_{in}=1.6°$ along [100] and [110]. The angular positions for selected spots are in good agreement with the calculations based on the Ewald concept (cf. Fig. 5). Note that the nomenclature $(g_1,g_2)_{[nm0]}$ refers to the direction $[nm0]$ of the primary electron momentum vector k_{in} in the surface plane. For all cases shown in Fig. 6, the primary momentum is parallel to the direction of the incident ion beam. The correct polar angles of the intensity spots and their dependence on electron energy provide clear-cut evidence for electron diffraction. This rules out the interpretation of preferential incoherent scattering discussed for the emission of secondary electrons after electron impact.[17]

Inspection of Figs. 3 and 4 reveals a weaker (11) spot for lower electron energies and for the resulting spot position closer to the surface normal. This is in line with the observation that spots could hardly be identified for emission of electrons at small polar angles, i.e., close to the direction of the surface normal (note the missing data points for small polar angles in Fig. 6). We interpret this finding by the electron emission process, where the primary excitation produces electrons which move parallel to the surface and are then scattered in single binary collisions from surface atoms under large angles into vacuum. The differential cross sections for scattering of electrons with energies in the 10–50 eV regime show maxima for forward and backward directions, but also a pronounced minimum around 90°,[18] i.e., for scattering along the surface normal.

The intensity spots observed here are clearly broader than the familiar sharp reflexes for well-prepared crystal surfaces investigated with conventional LEED using a fine-focused primary electron beam of defined energy. In order to explore

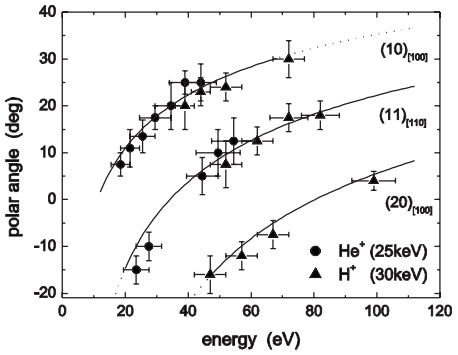

FIG. 6. Spot positions as a function of final electron energy for scattering of 25 keV He^+ ions (full circles) and 30 keV protons from Cu(001) under $\Phi_{in}=1.6°$ along [100] and [110]. Solid curves: results from modified Ewald construction; dotted parts of curves denote angles beyond acceptance of instrument.

the origin of the width of the diffraction spots, we performed detailed measurements for 25 keV He^+ ion impact on Cu(001) under $\Phi_{in}=1.8°$. For scattering of the incident ion beam along [100], we observe for electron energies in the interval from 20 to 25 eV, (22.5 ± 2.5) eV, the [10] reflex at polar angles around 12° with respect to this axis; whereas for ion impact along [110] this spot is shifted out of the acceptance of our instrument. For scattering along [110] the [11] spot can be detected at polar angles of about −15°, but for scattering along [100] this peak cannot be observed here (see Ewald construction in Fig. 5). In Fig. 7 we have plotted the intensity profiles along the directions of the projectile beam, where for scattering along [100] a pronounced peak at a polar angle close to the expected value of 12° is observed. By subtraction of the two data sets, we obtain the background corrected signal as a function of polar angle as shown in Fig. 8. We note that the peak signal is about 30% compared to the overall background signal.

For the analysis of the spot signal we describe the excited electrons in terms of a plane wave propagating parallel to the surface plane along [100] with wave vector k_{in} elastically scattered by lattice atoms arranged in strings with interatomic spacings $d=a/\sqrt{2}$. Taking into account the electronic surface potential V_o and exponential damping for the plane wave, one finds with $k_{out}=\sqrt{2E_e}$ and $k_{in}=\sqrt{2_e(E+V_o)}$ for the intensity of electrons emitted with energy E_e and elastic scattering from an infinite number of surface atoms (see also Ref. 10),

$$I = C/\{1 + e^{-d/\lambda} - 2e^{-d/2\lambda}\cos[d(k_{in} - k_{out}\sin\alpha)]\}, \quad (1)$$

where C is an instrumental factor, λ is the mean-free path, and the polar angle α is referred to as the surface normal.

The solid curve in Fig. 8 represents a best fit using Eq. (1) where also an averaging over the experimental interval of electron energies is performed. With $V_o=12$ eV for the Cu(111) surface,[16] we obtain from the fit $\lambda=24$ a.u. $=12.7$ Å. This value is fairly close to the mean-free path of electrons in metals which amounts for 20 eV electrons to about 10 Å.[19] Thus, the range of electrons in metals determines the (longitudinal) coherence length for propagation of

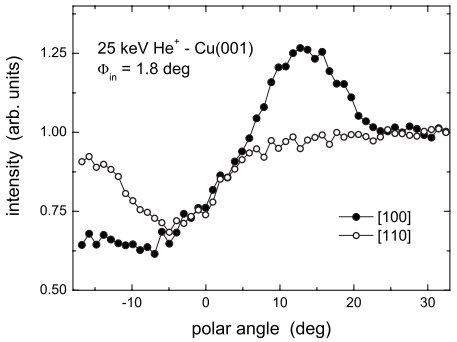

FIG. 7. Intensity for electrons with energies (22.5 ± 2.5) eV emitted during impact of 25 keV He^+ ions on Cu(001) under $\Phi_{in} = 1.8°$ along [100] (solid circles) and [110] (open circles) as a function of polar angle.

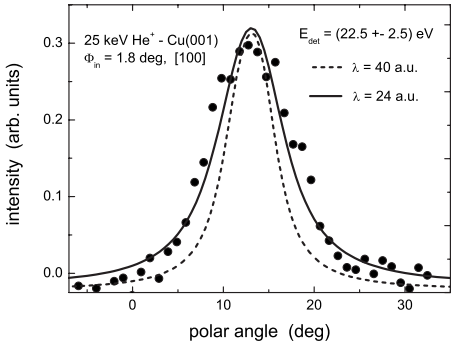

FIG. 8. Background corrected intensity for electrons with energies (22.5 ± 2.5) eV emitted during impact of 25 keV He^+ ions on Cu(001) under $\Phi_{in} = 1.8°$ [100] as a function of polar angle. Curves: calculations based on Eq. (1).

the excited electrons parallel to the surface. For comparison the dashed curve in Fig. 8 shows a calculation for $\lambda = 40$ a.u. $= 21$ Å which demonstrates the sensitivity of data on this parameter.

A further striking feature of our data is the presence of additional intensity spots in Figs. 3 and 4. These spots cannot be understood by electrons excited with a momentum along the [110] direction, i.e., parallel with respect to the incident ion beam; e.g., the angular positions of the two additional bright spots in Fig. 4 [labeled $(01)_{[120]}$ and $(10)_{[210]}$] compare well with the analysis based on the Ewald construction, if a preferential excitation of primary electrons takes place also along the [120] and [210] azimuth (dashed lines in Fig. 5). Further spots in Fig. 4 indicate that this type of channeling mechanism is an important feature for the production of fast electrons within the angular range of excitation in binary collisions with atoms. Such a mechanism has not been studied for this collision regime so far, and we hope that our work will stimulate theoretical treatments on this problem. This aspect is also relevant for an understanding of the transverse coherence in the scattering process which determines the width of the spots normal to the propagation of excited electrons. In passing, we note that a similar type of preferential electron excitation was observed for secondary electron scattering in crystals along low index directions which was explained by momentum matching in "interzone transitions."[17]

In conclusion, we have presented a detailed analysis of experiments on the emission of electrons with energies of some 10 eV by fast ions. The observed intensity spots in the angular distribution of these electrons are attributed to electron diffraction. Different from LEED, the primary electrons are produced in binary collisions between projectile ions and conduction electrons with a preferential propagation along low index strings of atoms in the surface plane. Ejection into vacuum proceeds via large-angle scattering with surface atoms, where a small differential cross section leads generally to a low electron intensity for emission around the surface normal. The longitudinal width of the spots is determined by a coherence length which directly relates to the electron mean-free path in metals. Fractions of such coherently scattered electrons amount to about 40%–50% of electrons emitted at those energies.

We hope that our work stimulates further experimental and theoretical studies on this interesting and important regime of electron emission. The relevance of such studies is related to the effects of electron diffraction on electron spectra, where structures or peaks for ion bombardment are interpreted in terms of basic physical processes as, e.g., Auger transitions or plasmon decay, but may originate for crystal surfaces from diffraction effects.[6,11]

Support from Deutsche Forschungsgemeinschaft (Project No. Wi 1336) is gratefully acknowledged. We thank Z. Fang for his assistance in the early stage of the measurements and H. von Hoegen (Essen) for helpful discussions.

*Author to whom correspondence should be addressed; winter@physik.hu-berlin.de

[1] K. Heinz *et al.*, Prog. Surf. Sci. **64**, 163 (2000).
[2] M. Henzler, Surf. Rev. Lett. **4**, 489 (1997).
[3] D. P. Woodruff and A. M. Bradshaw, Rep. Prog. Phys. **57**, 1029 (1994).
[4] M. Nègre *et al.*, Surf. Sci. **78**, 174 (1978).
[5] J. Mischler and N. Colombie, Surf. Sci. **40**, 311 (1973).
[6] T. Bernhard *et al.*, Phys. Rev. A **69**, 060901(R) (2004).
[7] R. A. Baragiola and C. A. Dukes, Phys. Rev. Lett. **76**, 2547 (1996).
[8] B. van Someren *et al.*, Phys. Rev. A **61**, 032902 (2000).
[9] N. Stolterfoht *et al.*, Phys. Rev. A **61**, 052902 (2000).
[10] A. Niehaus *et al.*, Nucl. Instrum. Methods Phys. Res. B **182**, 1 (2001).
[11] H. Eder *et al.*, Surf. Sci. **472**, 195 (2001); H. P. Winter *et al.*, Nucl. Instrum. Methods Phys. Res. B **182**, 15 (2001).
[12] U. Scheithauer *et al.*, Surf. Sci. **178**, 441 (1986).
[13] Omicron NanoTechnology, Taunusstein, Germany.
[14] A. van Hove *et al.*, *Low Energy Electron Diffraction* (Springer, Berlin, 1986).
[15] A. Hegmann *et al.*, Europhys. Lett. **26**, 383 (1994).
[16] E. V. Chulkov *et al.*, Surf. Sci. **437**, 330 (1999).
[17] J. Burns, Phys. Rev. **119**, 102 (1960).
[18] W. Williams and S. Traymar, Phys. Rev. Lett. **33**, 187 (1974).
[19] M. P. Seah and W. A. Dench, Surf. Interface Anal. **1**, 2 (1979).